Iranian Journal of Materials Science and Engineering, Vol. 18, Number 3, September 2021
RESEARCH PAPER

Structural, Dielectric and Electrical Properties of Modified $Bati_{0.80}Fe_{0.20}O_3$ Ceramics by Zr Addition in Ti Site at X=0.00 to 0.10.

Najwa Gouitaa *, Lamcharfi Taj-Dine, Abdi Farid and Ahjyaje Fatima Zahra

* *najwa.gouitaa@gmail.com*
Signals, Systems and Components Laboratory (LSSC), Electrical Engineering Department, University Sidi Mohamed Ben Abdellah USMBA, FST. Fez, Imouzzer Road B.P. 2202, Morocco

Received: January 2020 **Revised: March 2020** **Accepted: April 2020**
DOI: 10.22068/ijmse.2059

Abstract: *In this study, we have synthesized the Zr substituted $BaTi_{0.80}Fe_{0.20}O_3$ ceramics at different content of Zr from x=0.00 to 0.10 by using the solid-state route. The room temperature X-ray diffraction results confirmed the coexistence of the two tetragonal and hexagonal phases for $x \leq 0.050$ of Zr content. While above 0.050 the hexagonal phase disappeared in benefit of the tetragonal phase. The Raman results confirmed the formation of these phases obtained by XRD. The scanning electron micrographs consisted of both spherical and straight grain forms for x=0.000 to 0.075, and only spherical grain form for x=0.100 attributed to the tetragonal phase. Also, the grain size increased accompanied by a decrease in density of ceramics with increasing Zr content up to 0.050 then decreased accompanied by an increase in density. Detailed studies of dielectric permittivity measurement provided a presence of two anomalies T_e and T_{R-O} at different temperatures, with a relaxation phenomenon and diffuse behavior which was very important for ceramic at x=0.075 of Zr content. The dielectric permittivity values of the two anomalies of Zr substituted $BaTi_{0.80}Fe_{0.20}O_3$ ceramics increased with the increase of Zr content and the dielectric loss was minimal at x=0.100 of Zr content. The conductivity increased with increasing of Zr substitution from 0.025 to 0.075 levels while for x = 0.100 the dielectric conductivity decreased. And the Cole-Cole analysis indicated a negative thermal resistivity coefficient (NTCR) behavior of these materials and ideal Debye-type behavior.*

Keywords: *Solid-state, X-ray diffraction, Raman, dielectric permittivity, anomalies, relaxation, diffuse, conductivity, Cole-Cole.*

1. INTRODUCTION

In the ferroelectric family, barium titanate ($BaTiO_3$) is the most widely used ferroelectric material, and, even after seventy-five years of its discovery, it remained an essential material with excellent dielectric [1, 2], optical [3], piezoelectric [4], and ferroelectric [5] properties. In addition, it is one of the most studied lead-free ferroelectric materials due to its wide range of applications, namely: capacitors, transducers, non-volatile memories, positive temperature coefficient (PTC) thermistors, and many others [6-9]. The high dielectric constant and low dielectric loss make it one of the most popular candidates for dynamic random-access memory (DRAM) and tunable microwave device applications [10-12]. The technological importance has triggered many studies on multiferroic materials, exhibiting both dielectric and magnetic properties by modifying or improving their properties by different dopants or different conditions. In this perspective, the $BaTiO_3$ ceramic was dopped with ions of the transition metals such as Fe^{3+} in the Ti site. It is found by many researchers that the Fe-$BaTiO_3$ substitution leads to the formation of hexagonal phase which became predominant for high levels of Fe [13].

The (Ba (Zr_yTi_{1-y}) O_3, BZTs) ceramics can be formed by the replacement of Ti^{4+} by Zr^{4+} in the B-site of the $BaTiO_3$ lattice. The BZTs ceramics with y = 0.05–0.08 have a high dielectric constant ($\varepsilon > 13{,}000$) with low loss tangent ($\tan\delta < 0.05$) [14, 15]. For BZTs compositions of $0<y<0.15$, phase transition temperatures occur for rhombohedral to orthorhombic (T_1), orthorhombic to tetragonal (T_2), and tetragonal to cubic (T_c). The phase transitions are strongly dependent on the amount of Zr. When the Zr concentration is about 15 at. %, the three-phase transition temperatures merged into a single diffuse phase transition [16].

Many researchers have reported that solid solutions between BZTs and other multiferroic materials showed many interesting properties. For example, Jha et al. reported that the $BaZr_{0.025}Ti_{0.975}O_3$–$BiFeO_3$ system exhibited a relaxor multiferroic [17] and C. Kruea-In and al have reported a diffuseness and relaxation behavior of $Ba(Zr_{0.05}Ti_{0.95})_{1-x}(Fe_{0.5}Ta_{0.5})_xO_3$ ceramics [18].

[DOI: 10.22068/ijmse.2059]

In the previous works, it was found that the Fe-$BaTiO_3$ (BTF) substitution stabilizes the hexagonal phase at high content of Fe and decreases the dielectric properties of $BaTiO_3$ ceramics [19, 20]. This is why it is interesting to modify the dielectric properties of BTF by co-doping on-site A or on B site of $BaTiO_3$ to their adaptations to very specific applications. This is the context of this study consisting of the study of structural and dielectric properties of Zr substituted $BaTi_{0.80}Fe_{0.20}O_3$ ceramics at Ti-site for x=0.00 to 0.10.

2. EXPERIMENTAL

The $BaTi_{0.80}$-x$Fe_{0.20}ZrxO_3$ (BZ_xTF) ceramics for x=0.00 to 0.10 were prepared by the conventional solid-state method using the high-purity oxides $BaCO_3$, TiO_2 ZrO_2, and Fe_2O_3. These oxide powders were weighted in stoichiometric proportion and milled under acetone for 4h. After that, the powders were dried at 80 °C for 24h. The dried powders were ground using agate mortar for 30 min and then de-carbonated and pre-reacted by calcining in alumina at 1100 °C for 4h. After calcination, the powders were ground for 30 min. The structure, phase purity, and lattice parameters of the product were characterized by X-ray diffraction (XPERT-PRO with Cu Kα radiation with λ=1.5406Å), and the Raman spectrum was recorded at room temperature.

To form the pellets for scanning electron microscope (SEM) and dielectric measurements, the calcined powders were mixed with a few drops of 1 wt% Polyvinyl Alcohol (PVA) as a binder then pressed using uniaxial pressing. The pellets formed were sintered in air at 1200°C for 6h. The investigations of the microstructure of the pellets were performed using SEM. And the dielectric properties as a function of frequency and temperature were studied with Agilent E4980A (20 Hz-2 MHz).

3. RESULTS AND DISCUSION

3.1. X-ray diffraction results

The Figure 1.a shows the X-ray diffraction patterns for BZ_xTF powders for x = 0.000, 0.025, 0.050, 0.075, 0.100 calcined at 1100 ° C for 4h. The spectra of the powders at x = 0.000, 0.025, and 0.050 show the presence of the characteristics of the peak of the tetragonal phase as well as those of the hexagonal phase. And beyond 0.050, the peaks of the hexagonal phase disappear completely, and only these of the tetragonal phase remains. In addition, all the compositions have a pure perovskite structure without the presence of a secondary phase. This indicates that the Zr and Fe are well incorporated into the BTO to form a homogeneous solid solution.

To study the influence of Zr on the evolution of the phase structure of the BTFO, we have zoomed on the most intense peaks (101) and (104) of the two tetragonal and hexagonal phases respectively (Figure 1.b).

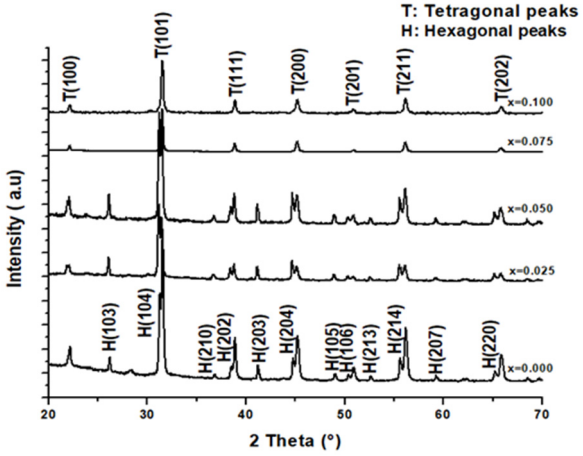

(a)

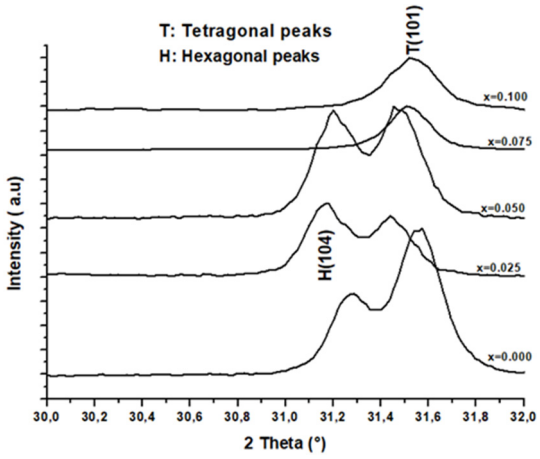

(b)

Fig. 1. a. X-ray diffractogram of BZxTF powders for x = 0.000, 0.025, 0.050, 0.075, 0.100 b. Zoom on T (101) et H(104) peaks characteristic of tetragonal and hexagonal phase respectively.

For x = 0.00 these two peaks are distinguished and when the rate of Zr increases, the intensity of the tetragonal peak (101) achieved a minimum at x = 0.025 then decreases while the intensity of the hexagonal peak (104) increases and becomes of the same intensity as the tetragonal peak (101) at

[DOI: 10.22068/ijmse.2059]

x = 0.075 then disappears beyond this rate, thus indicating the presence only of the tetragonal phase. Therefore, the substitution of BTFO by Zr stabilizes the tetragonal phase for Zr rates greater than 0.075. We notice that the position of the two diffraction peaks (101) tetragonal and (104) hexagonal is shifted towards the small angles for x = 0.025 and 0.05 then towards the high angles for x = 0.075 and 0.100. The shift of the peak towards the small angles is may be due to the crystal distortion induced by the fact that the ionic radius of Zr^{4+} (0.72Å) is greater than that of Ti^{4+} (0.605Å).

The values of the lattice parameters of the $BaTiO_3$ powders co-substituted with Zr and Fe, for the tetragonal and hexagonal phase, are grouped in Table.1. They are calculated using the "Unit Cell" software based on the values of the intensities and the positions of the peaks of each phase in XRD. The results are shown in Figure.2. These graphs show that the parameters a and c as well as c / a (tetragonality) decrease and reach a minimum at Zr = 0.05 then increase.

We also note that the lattice parameters a and c of the hexagonal phase decrease with the increase in the rate of Zr up to x = 0.025 and then increase to 0.05 (see Table 1).

The increase in parameters and tetragonality is due to the presence of Zr^{4+} ions with an ionic radius (r_i (Zr^{4+}) = 0.72Å) greater than the ionic radius of titanium (ri (Ti^{4+}) = 0.605 Å). We can also note that, unlike the effect of Fe on $BaTiO_3$ [19], the Zr co-substitution disappears the hexagonal phase and stabilizes the tetragonal phase beyond 0.075, which leads to an increase in tetragonality at these levels of substitution.

3.2. Raman results

The Figure 3 shows the Raman spectra in the frequency region of 100-1000 cm^{-1} of BZ_xTF powders for x = 0.000, 0.025, 0.050, 0.075, 0.100. These spectra are adjusted using the peak fit software as shown in Figure 4 and all the parameters of the position of each band and the corresponding width at half height (FWHM) are reported in Table.2.

From Figure 3, the BZ_xTF at x = 0.00, shows the existence of the characteristic bands of the hexagonal phase in particular that around 680 cm^{-1}. By substituting the BTFO with the Zr at x = 0.025 and 0.050, this band still exists but decreases in intensity and shifts towards the low frequencies (see Figures 3 and Table 2), thus indicating the enhancement of the hexagonal phase for these rates of Zr. Such phenomena of shifting of the Raman spectrum are attributed to the variation of chemical environments and of stresses [21].

Table 1. Unit cell parameters of the tetragonal and hexagonal phase of BZxTF powders for x = 0.000, 0.025, 0.050, 0.075, 0.100.

Zr content	Unit cell parameters (Tétra.)	Unit cell parameters (Hexa.)
0.000	a=b=4.00668 c=4.03009	a=b=5.839 c=13.7607
0.025	a=b=4.00510 c=4.01420	a=b=5.634 c=13.556
0.050	a=b=4.00478 c=4.00960	a=b=5.682 c=13.610
0.075	a=b=4.00604 c=4.0209	
0.100	a=b=4.00640 c=4.0258	

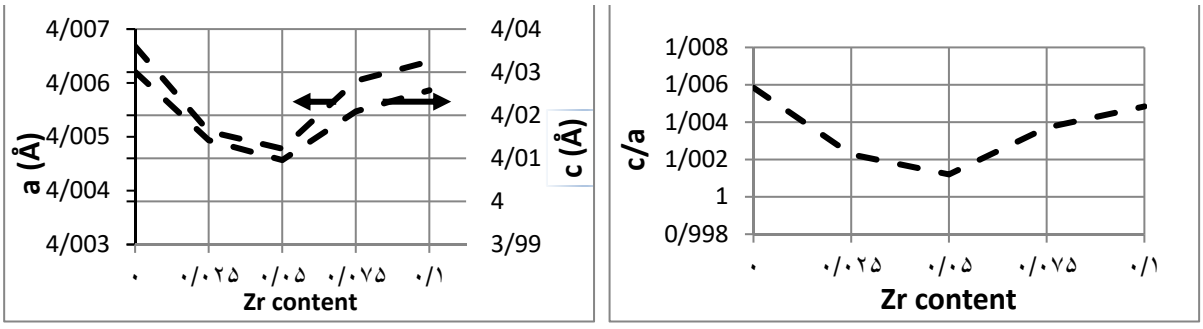

Fig. 2. . Evolution of a, c and c/a parameters of BZxTF powders for x = 0.000 to 0.100.

[DOI: 10.22068/ijmse.2059]

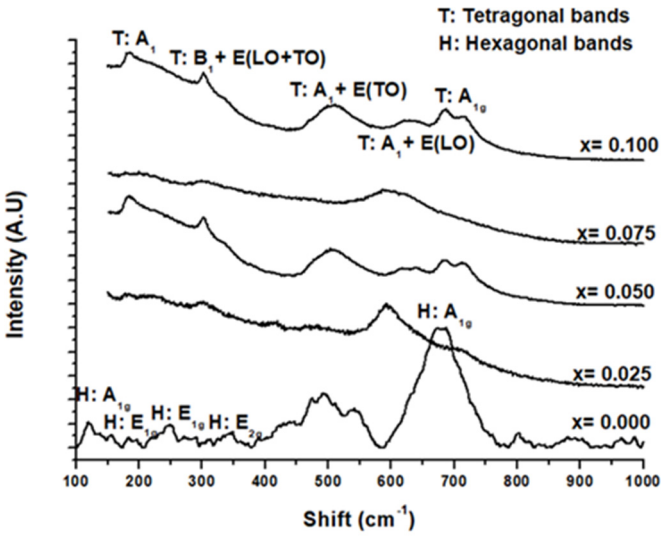

Fig. 3. Raman spectra of $BaTi_{0.8-x}Zr_xFe_{0.2}O_3$ powders for x = 0.000, 0.025, 0.050, 0.075, 0.100

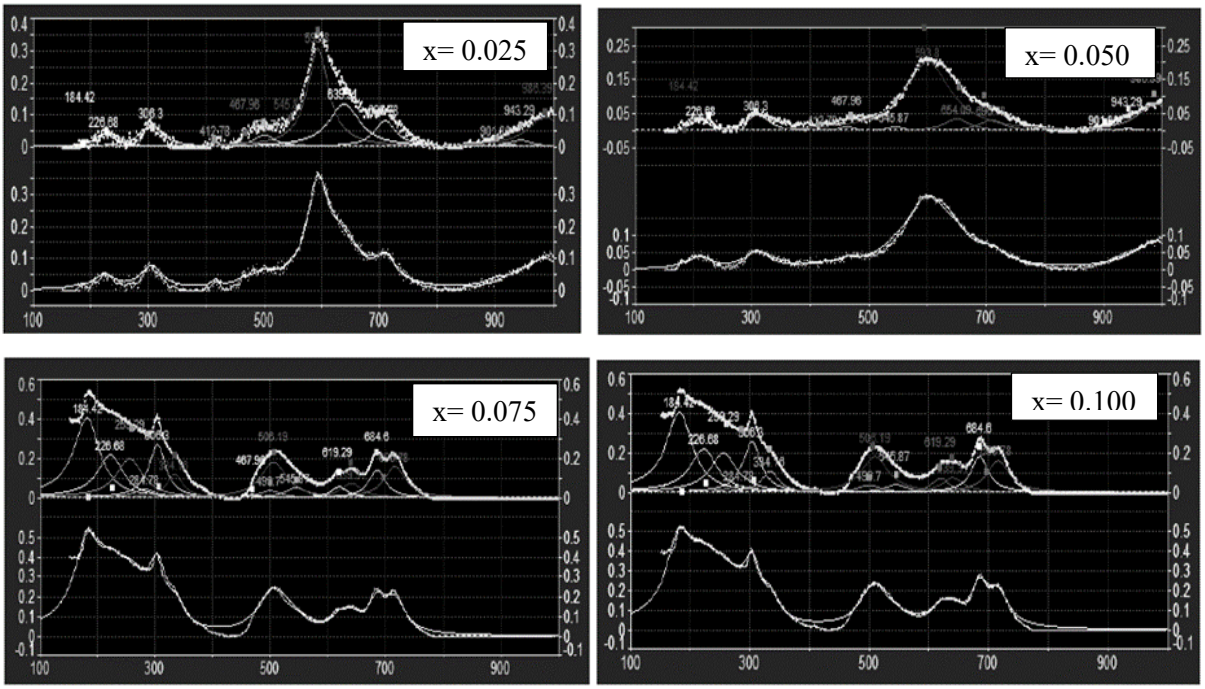

Fig. 4. Peakfit ajustement for BZxTF ceramics for x= 0.025, 0.050, 0.075, 0.100.

Table 2. Shift Raman and FWHM parameters of BZxTF ceramics for x=0.000, 0.025, 0.050, 0.075, 0.100.

	Shift Raman (cm^{-1})				**FWHM**			
bands	x= 0.025	x= 0.05	x= 0.075	x=0.10	x=0.025	x=0.050	x=0.075	x=0.10
A_1	184	184	186	186	35	35	55	55
B_1+E(LO+TO)	306	310	304	304	45	50	35	35
A_1+ E(TO)	500	500	545	545	45	45	45	45
A_{1g}	639	650	640	640	65	55	45	45
A_1+E(LO)	709	709	716	716	45	55	45	45

[DOI: 10.22068/ijmse.2059]

The spectrum of BZ_xTF powder at x = 0.075 and 0.100 were fitted with five main modes at 183, 306, 500, 640 and 716 cm^{-1}. Indeed, the band at 306 cm^{-1} and the wider asymmetric bands at 505 and 640 cm^{-1} correspond well to the tetragonal phase [20]. In addition, the peaks around 500 and 640 cm^{-1} correspond to the phonon vibrations of the Ba-O bonds, while the peaks at 183 and 303 cm^{-1} correspond to the phonon vibrations of the Ti-O bonds. It should be mentioned that the intensity of the peak around 500 cm^{-1} increases for x = 0.075 and 0.10 thus indicating a dominance of the tetragonal phase at these compounds. In addition, the positions of the bands and the width at mid-height (FWHM) at these substitution rates are the same, which confirms the stability of the tetragonal phase at these Zr substitution rates determined also by the XRD.

The vibrations in the Raman patterns which have a splitting suggest that the structural disorder results from the distortion of the lattice. The splitting of the band at 716 cm^{-1} of the co-substituted ceramics suggests the presence of a higher disorder compared to pure $BaTiO_3$. The significant shift of the peak at 500 cm^{-1} towards a higher frequency (545 cm^{-1}), with the increase in the rate of Zr, is expected due to the difference in ionic radius between Ti^{4+} and Zr^{4+}, which results in the network distortion and widening of the energy band. The Raman spectrum of the two tetragonal and hexagonal phases for x less than 0.05, relates to the existence of the two bands at 505 cm^{-1} (tetragonal) and 680 cm^{-1} (hexagonal), hence the coexistence of these two phases at these rates of Zr. These results of the Raman spectroscopy study agree well with those of the XRD.

The values of the grain size are grouped in Table 3 and it is observed that it increases with Zr substitution and reach a maximum at 0.05, then decreases for the other rates of Zr. The increase in grain size for x<0.50 of Zr content is due to the coexistence of the two phases while the decrease in the latter for high levels of Zr is related to the effect of Zr which decreases grain size [21].

The relative density values of the BZxTF ceramics are grouped in Table 3. We note that for Zr levels less than 0.05, the density decreases with increasing Zr content. On the other hand, for the levels higher than x = 0.05 the density of the ceramics increases. The decrease in density can be attributed to the presence of grains of different shapes (coexistence of the two tetragonal and hexagonal phases) while the increase in density is probably due to the presence of grains of homogeneous shape linked to the phase tetragonal.

3.3. Dielectric properties

The dielectric constant as a function of temperature for BZ_xTF ceramics (x = 0.00, 0.025, 0.050, 0.075 and 0.100) is shown in the Figure. 5. The dielectric permittivity evolution as a function of temperature for x = 0.00, shows an anomaly around 300°C attributed to the phase transition from the rhombohedral phase to the orthorhombic phase T_{R-O} [23]. This transition presents a diffuse character and the value of the maximum of $\varepsilon'_{r,\,max}$ remains almost quasi-constant in a temperature interval of about 100°C (Figure 6. c and d). In addition, this maximum shifts towards high temperatures with increasing frequency, indicating a relaxation behavior. For the other substitution rates, the change in dielectric permittivity as a function of temperature is isotypic to that at x = 0.00 but the transition temperature depends on the rate of substitution in Zr. Another anomaly is present around T_e =150 °C for x = 0.00, 0.025, and 0.075 of Zr contents which is related to the transition temperature from the ferroelectric phase to the paraelectric phase of pure $BaTiO_3$ [18].

Analysis of all these ceramics indicates that the dielectric permittivity at low frequencies is greater than that obtained at high frequencies.

Table 3. Average grains size and density values of BZxTF ceramics for x=0.000, 0.025, 0.050, 0.075, 0.100.

Zr content	Average grains size (µm)	Density (%)
0.000	1,478	89
0.025	1,523	86
0.050	1,64	78
0.075	1,589	81
0.100	1,492	83

[DOI: 10.22068/ijmse.2059]

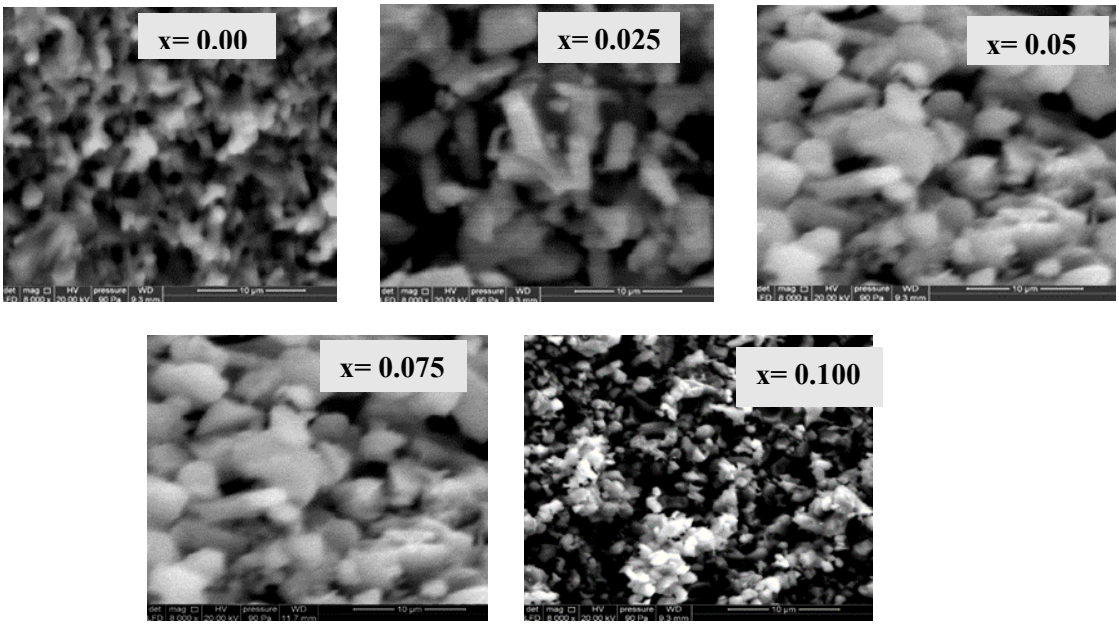

Fig. 5. Micrographs SEM of BZxTF ceramics for x= 0.000, 0.025, 0.050, 0.075, 0.100.

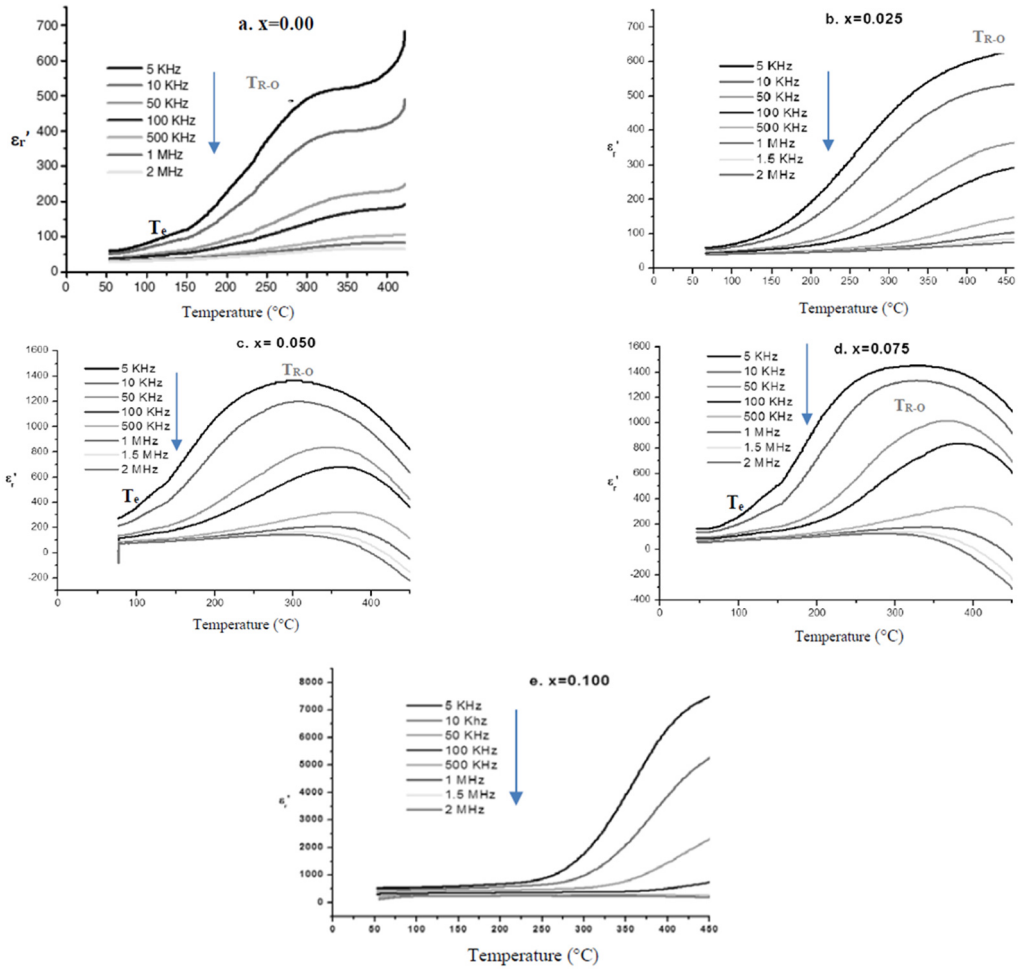

Fig. 6. Temperature dependence of dielectric permittivity of BZxTF ceramics for x=0.000, 0.025, 0.050, 0.075, 0.100.

[DOI: 10.22068/ijmse.2059]

The decrease in dielectric permittivity is due to the dipoles which cannot follow the alternation of the applied electric field which obtains higher frequencies, then the total polarization of the orientation will be less at the higher frequencies.

The two anomalies T_{R-O} and T_e exhibit a relaxation phenomenon and diffusion behavior for all the ceramics co-substituted with Fe and Zr. It is known that the compositional disorder exists in the B site of the $BaTiO_3$ ceramic with the co-substitution of two ions of Fe^{3+} and Zr^{4+}. This compositional disorder disrupts long-range order correlations, thus leading to the formation of polar nano-regions (PNRs) [24] and this relaxation behavior can be attributed to PNRs. In addition, the diffuse character may be attributed to cationic disorder and composition fluctuation induced by site substitutions of Ti by two ions of Fe and Zr [25]. The values of the temperatures T_e and T_{R-O} as well as the maximum dielectric permittivity $\varepsilon'_{e,max}$ and $\varepsilon'_{R-O,max}$, corresponding to these temperatures respectively, for a frequency fixed at 5 kHz are grouped in Table 4. We notice that the temperature of T_e anomaly moves towards low temperatures with the increase of Zr for x = 0.050 and 0.075 and it is no longer observed for x = 0.025 and 0.100 probably due to the widening of the peak of this anomaly. This peak broadening may be attributed to the merging of two types of transitions, and/or structural heterogeneity. The same shift in the transition temperature T_e has been reported by A. Elbasset et al [22] for Zr substituted $BaTiO_3$ ceramics. While the T_{R-O} phase transition, it moves towards high temperatures for x = 0.025, 0.075, and 0.10 and towards low temperatures for x = 0.050. This abnormal evolution of the T_{R-O} temperature as a function of the Zr rate is probably due to the presence of Fe^{3+} ions which substitute the Ti site with the Zr which disturbs the displacement of the phase transition with the substitution for the Zr.

We also notice, from table 4, that the maximum of the dielectric permittivity of T_e anomaly ($\varepsilon'_{e,max}$) presents a maximum value at x = 0.05 then decreases for x = 0.075 of Zr. The same evolution of ε'_{max} as a function of the Zr- $BaTiO_3$ substitution has been reported by A. Dixit et al 26. While the maximum dielectric permittivity $\varepsilon'_{R-O,max}$ increases with the increase of Zr substitution and reaches a maximum of 7500 at x = 0.100.

The evolution of the dielectric losses of $BaTi_{0.80-x}Zr_xFe_{0.20}O_3$ (x = 0.00, 0.025, 0.050, 0.075 and 0.100) ceramics as a function of temperature from the ambient at 450°C is shown in the Figure. 7. The graphs show different anomalies depending on the Zr substitution rate. For x = 0.00 and 0.025 we notice a slight increase in dielectric losses at 200°C followed by a significant increase with temperature until reaching a maximum value around the temperature of 450°C. The intensity of this maximum decreases with the frequency. And for x = 0.050 and 0.075, the dielectric losses are almost constant for low temperatures then reach a maximum around 400°C. This maximum moves towards the lower temperatures with frequency and also decreases in intensity. While at x = 0.010, the evolution of dielectric losses as a function of temperature in particular. Indeed, the latter increase with the temperature until reaching a maximum at 250°C for 5 KHz frequency, then they decrease.

These maxima are characterized by a very dispersive pattern for all frequencies, moreover, they move towards high temperatures with increasing frequency.

We also note that the value of the dielectric loss increases with the co-substitution of BTFO with Zr for the rates of x = 0.025 to 0.075. While for x= 0.010 the loss angle is minimal, so this is the optimal rate of substitution in Zr to have the least dielectric loss with the greatest value of dielectric permittivity.

The effect of Zr co-substitution on the conductivity of BTFO ceramics can be studied by measuring the alternating conductivity. Thus, the frequency-dependent electrical conductivity was calculated at different temperatures ranging from ambient to 450°C, for all co-substituted components of BZ_xTF (x = 0.00, 0.025, 0.050, 0.075, and 0.100) as shown in the Figure. 7.

It is clear from Figure 7 that the conductivity increases with frequency and temperature. A dispersion in conductivity was observed at lower frequencies for temperatures above 310°C for all samples co-substituted with Zr. While for temperatures below 310°C, the conductivity curves are merged indicating less mobility of defects. The plateau region is observed in the low-frequency region (frequency-independent conductivity, i.e. continuous conductivity σ_{dc}) and this frequency region increases with increasing temperature. This is observed for all the samples co-substituted with Zr. It is clear that the Zr substitution at 0.025 to 0.075 levels, increases the alternating conductivity.

[DOI: 10.22068/ijmse.2059]

Table 4. T_e, T_{R-O}, ε'_e and ε'_{R-O} values at different Zr content.

Zr content	T_e	$\varepsilon'_{e,max}$	$T_{R-O,max}$	ε'_{R-O}
0.00	127	103	280	510
0.025	---	---	458	631
0.05	110	410	296	1370
0.075	109	310	321	1460
0.10	---	---	450	7492

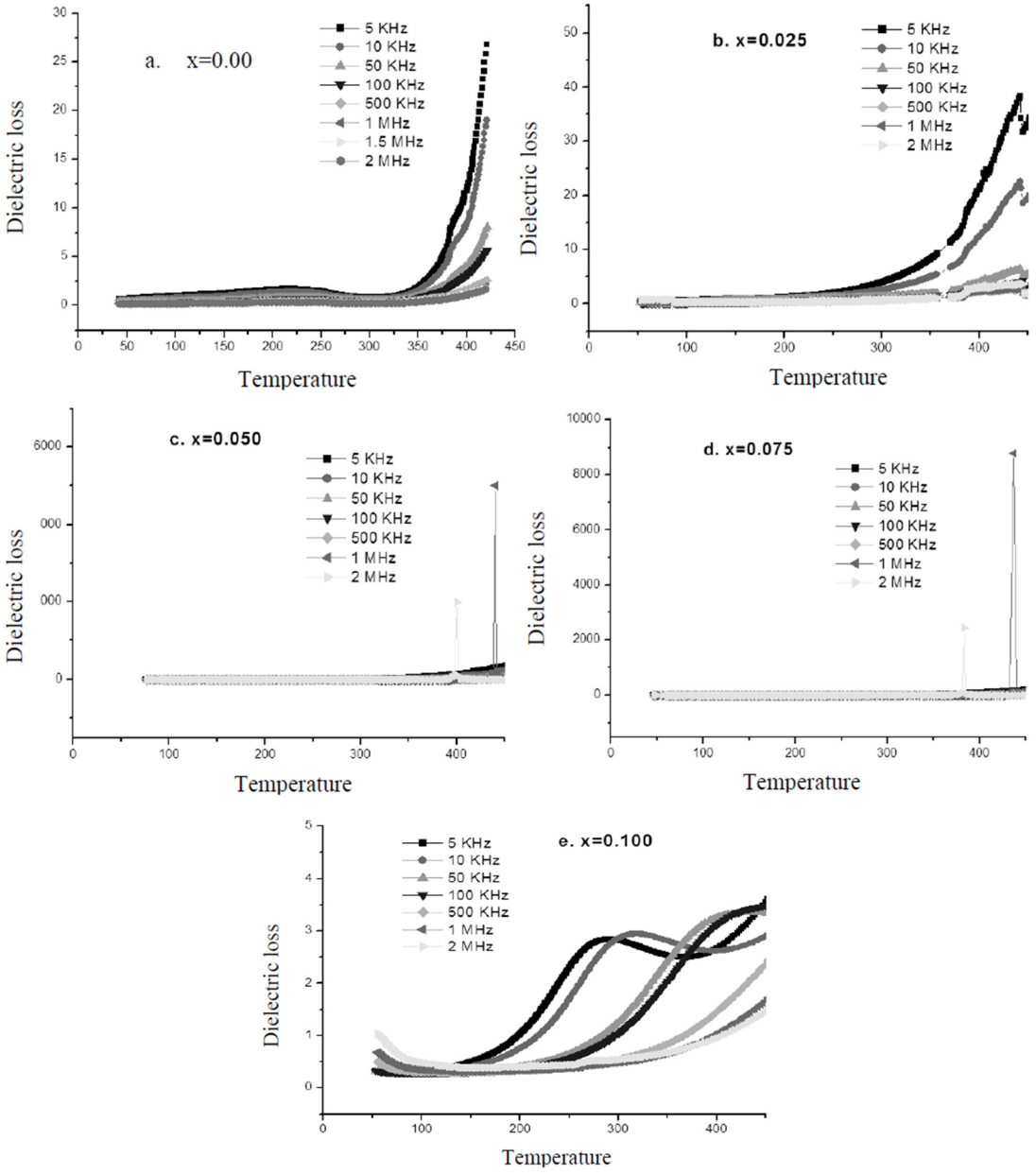

Fig. 7. Temperature dependence of dielectric loss of BZxTF ceramics for x=0.000, 0.025, 0.050, 0.075, 0.100.

[DOI: 10.22068/ijmse.2059]

While for x = 0.100 the dielectric conductivity decreases, this is due to the Zr ion co-substitution which is chemically more stable that reduces the electron jump between Ti^{4+} and Ti^{3+}, thus increasing the resistivity of these materials [27].

The complex impedance spectroscopy is known to be a powerful tool for separating the effect of grain and grain boundaries [28, 29]. It is used to study the electric properties in the material [31, 32]. To confirm the formation of barrier layers in the BZ_xTF ceramics, we analyzed the complex impedance using the Cole - Cole plot. Figure 8

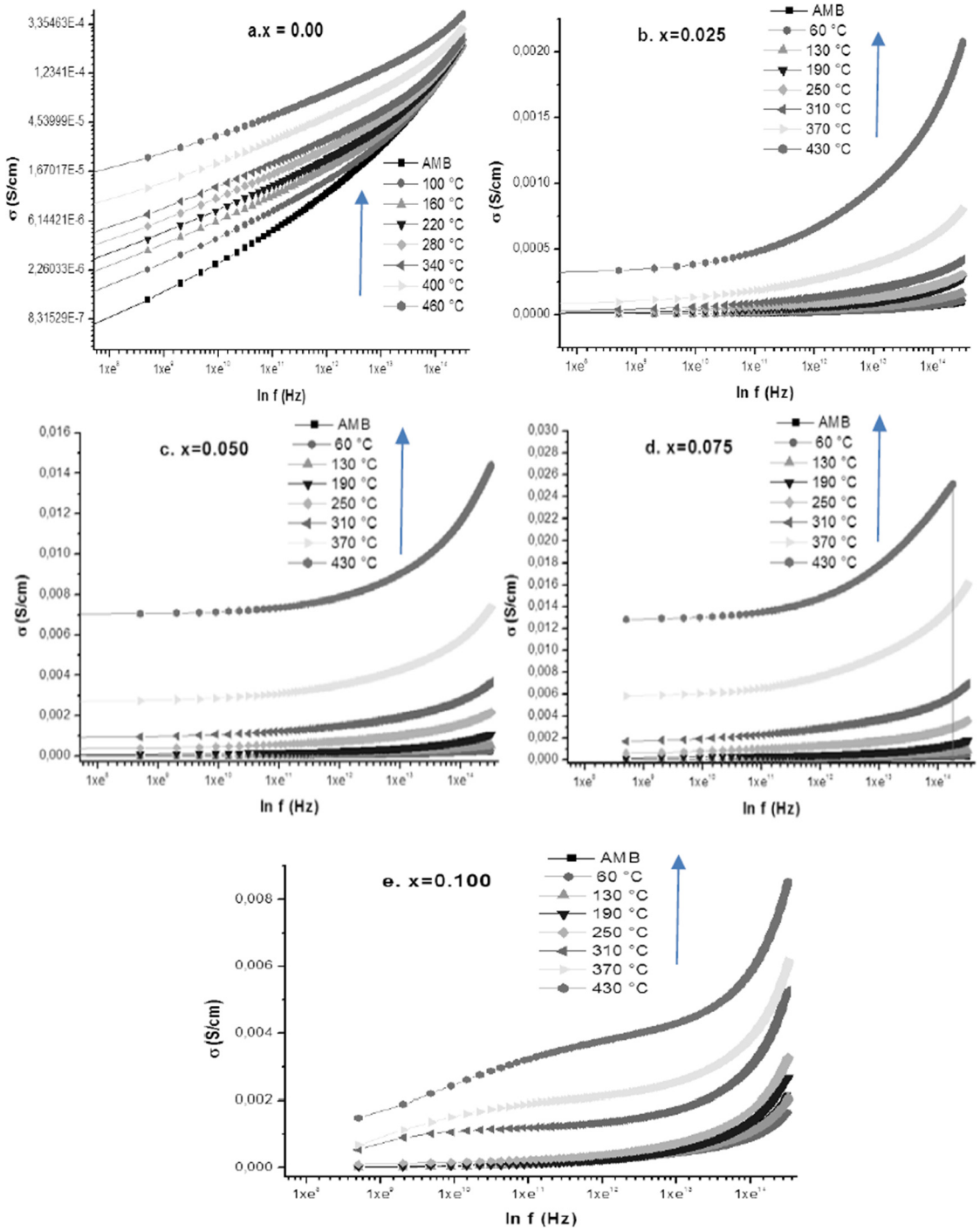

Fig. 8. Conductivity evolution as function of frequency at different measurement temperatures of BZ_xTF ceramics (x= a. 0.00, b. 0.025, c. 0.050, d. 0.075 et e. 0.100).

[DOI: 10.22068/ijmse.2059]

shows the variation of the imaginary part of the impedance (Z '') as a function of the real part (Z ') (Cole - Cole plots) at different temperatures of BZ_xTF sintered samples. These graphs show the presence of a semicircular arc. The radius of this arc formed by the intercept points on the real axis shift towards the origin as the temperature increases, indicating the decrease in the. resistive property of these materials [26]. The semicircular is fitted using the parallel combination of resistance-capacitance (R-C) and (R-CPE) circuits connected in series as shown in the inset of Figure 9.b. The radii of all these ceramics decrease with the increase in the temperature, which indicates a negative thermal resistivity coefficient (NTCR) behavior of these materials, generally found in the case of semiconductors. The center of the arcs is above the x-axis for co-substituted ceramics, thus showing ideal Debye-type behavior.

At x = 0.100, we can see the start of the appearance of a second arc at high temperature. The lower frequency arc corresponds to the grain boundary, while the higher frequency arc corresponds to a grain [28, 29]. This confirms the formation of barrier layers in this sample at high temperature [32].

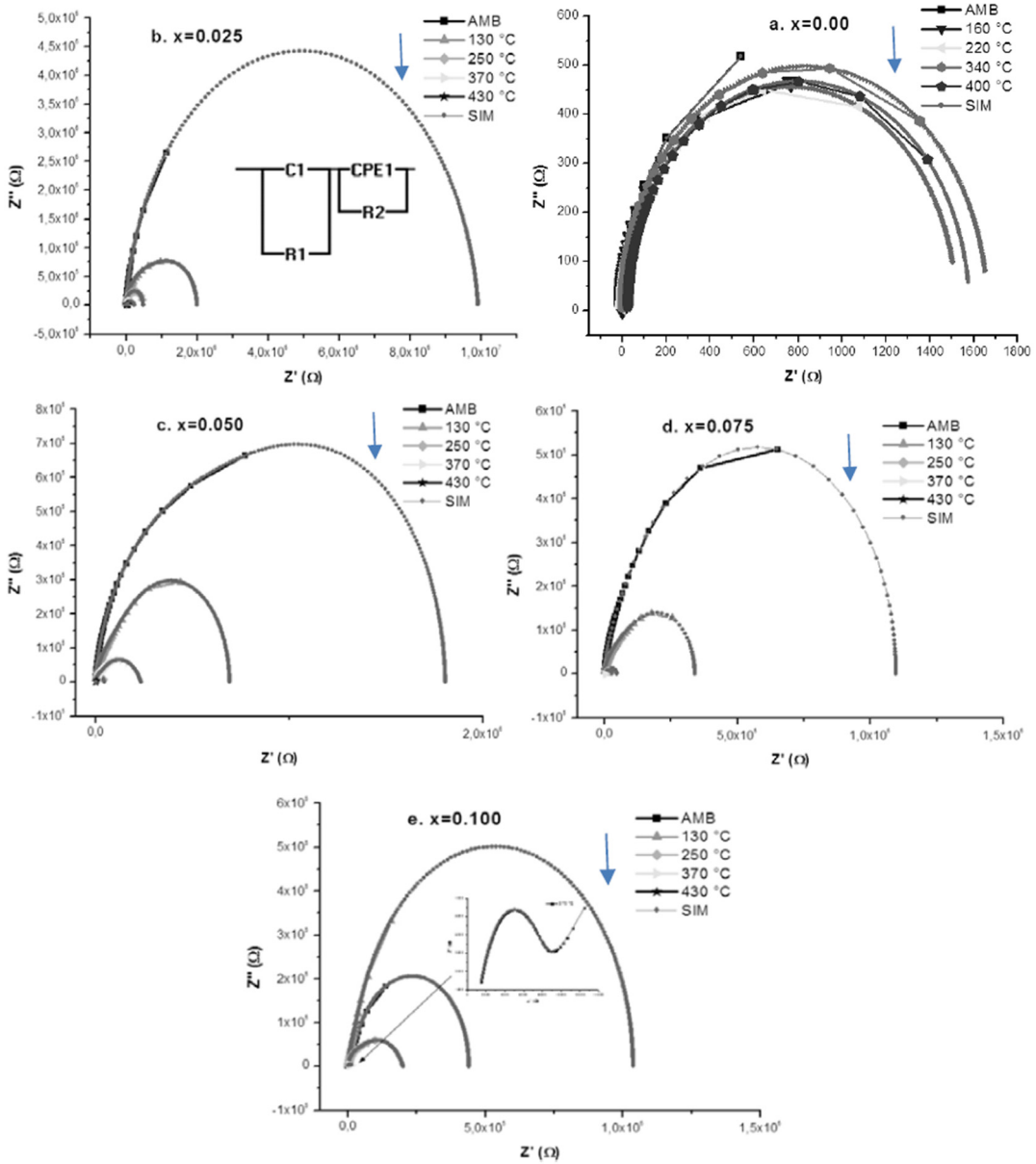

Fig. 9. Cole-Cole diagram at different measurement temperatures of BZ_xTF ceramics (x= a. 0.00, b. 0.025, c. 0.050, d. 0.075 et e. 0.100).

[DOI: 10.22068/ijmse.2059]

4. CONCLUSION

The BZ_xTF ceramics were successfully synthesized by the solid-state method. The XRD results confirmed the coexistence of tetragonal and hexagonal phases for $x \leq 0.050$. While at x=0.075 and 0.100, the hexagonal phase disappeared and only the tetragonal phase is present. The SEM results, of the pellets sintered at 1200°C for 6 h, showed a spherical and straight grain form for x = 0.000 to 0.075, and for x=0.100 the grain form was mostly spheric. And the density of these pellets decreased with increasing Zr content for $x \leq 0.5$, while above this content the density increased. The evolution of dielectric properties as a function of temperature showed the existence of two phases transition T_e, T_{R-O}, and the dielectric permittivity of Zr co-substituted BTF were improved compared with BTF ceramics. These phases' transition showed a relaxation phenomenon and a diffuse behavior which was very important for BZ_xTF ceramics at x= 0.050 and 0.075 for T_{R-O} phase transition. At x= 0.100, the dielectric properties were improved. However, the dielectric permittivity was maximal and the dielectric loss was minimal at this rate of Zr. The electric properties study showed a decrease of conductivity for x= 0.025 to 0.075 of Zr content and an increase of this conductivity for x= 0.100. While the cole-cole measurement indicated a NTCR behavior of these materials and ideal Debye-type behavior.

5. REFERENCES

[1] Li, W, Xu, Z, Chu, R, Fu, P, Zang, G. Structural and dielectric properties in the (Ba1− x Cax) ($Ti_{0.95}$ $Zr_{0.05}$)O_3 ceramics. Current Applied Physics, 2012, 12, 748-751.

[2] Pecharroman, C, Esteban-Betegon, F, Bartolome, J.F, Lopez-Esteban, S, Moya, J.S. New Percolative $BaTiO_3$–Ni Composites with a High and Frequency-Independent Dielectric Constant ($\epsilon r \approx$ 80000). Advanced Materials, 2001, 13, 1541-1544.

[3] Woldu, T, Raneesh, B, Sreekanth, P, Reddy, M.R., Philip, R, Kalarikkal, N. Size dependent nonlinear optical absorption in $BaTiO_3$ nanoparticles. Chemical Physics Letters, 2015 625, 58-63.

[4] Wang, Z, Suryavanshi, A.P, Yu, M.-F. Ferroelectric and piezoelectric behaviors of individual single crystalline $BaTiO_3$ nanowire under direct axial electric biasing. Applied physics letters, 2006, 89 - 082903.

[5] Bersuker, I. On the origin of ferroelectricity in perovskite-type crystals. Physics Letters, 1966 20, 589-590.

[6] Sette, D, Kovacova, V, Defay, E. Printed Barium Strontium Titanate capacitors on silicon. Thin Solid Films, 2015, 589, 111-114.

[7] Jin, X, Sun, D, Zhang, M, Zhu, Y, Qian, J. Investigation on FTIR spectra of barium calcium titanate ceramics. Journal of electroceramics, 2009, 22, 285-290.

[8] Capurso, J.S, Alles, A.B, Schulze, W.A. Processing of Laminated Barium Titanate Structures for Stress-Sensing Applications. Journal of the American Ceramic Society, 1995, 78, 2476-2480.

[9] Qi, J, Gui, Z, Wang, Y, Zhu, Q, Wu, Y, Li, L. The PTCR effect in $BaTiO_3$ ceramics modified by donor dopant, Ceramics international, 2002, 28, 141-143.

[10] Lin, F, Jiang, D, Ma, X, Shi, W. Influence of doping concentration on room temperature ferromagnetism for Fe-doped $BaTiO_3$ ceramics. Journal of Magnetism and Magnetic Materials, 2008, 320, 691-694.

[11] Lin, Y.H, Zhang, S, Deng, C, Zhang, Y, Wang, X, Nan, C.W. Magnetic behavior and thickness dependence in Co-doped BaTiO3 thin films. Applied Physics Letters, 2008, 92. 116.

[12] Cho, Y, Hyun, T, Choi, S. Microwave dielectric properties of ferroelectric BaTiO3 thin film. Journal of electroceramics, 2004, 13, 251-255.

[13] Dang, N. V, Thanh, T. D, Hong, L. V, Lam, V. D, and Phan, T.L. Structural, optical and magnetic properties of polycrystalline $BaTi_{1-x}Fe_xO_3$ ceramics. Journal of Applied Physics, 2011, 110(4): 043914-043914-7.

[14] Yu, Z, Guo, R, Bhalla, A.S. Dielectric behavior of $Ba(Ti_{1-x}Zr_x)O3$ single crystals. J. Appl. Phys, 2000, 88, 410.

[15] Rout, S.K, Cavalcante, L.S, Sczancoski, J.C, Badapanda, T, Panigrahi, S, Siu Li, M,

[DOI: 10.22068/ijmse.2059]

Longo, E. Photoluminescence property of $BaZr_{0.25}Ti_{0.75}O_3$ powders prepared by solid state reaction and polymeric precursor method. Physica B 404, 2009, 3341–3347.

[16] Yu, Z, Ang, C, Guo, R, Bhalla, A.S. Dielectric properties of $Ba(Ti_{1-x}Zr_x)O_3$ solid solutions. Mater. Lett, 2007, 61, 326.

[17] Jha, P.A, Jha, P.K, Jha, A.K, Dwivedi, R.K. Phase transformation and two-mode phonon behavior of (1 − x) [Ba $Zr_{0.025}Ti_{0.975}O_3$]–(x) [$BiFeO_3$] solid solutions. Journal of Alloys and Compounds, 2014, 186-192.

[18] Kruea-In, C, Rujijanagul, G. Electrical properties and phase transition of $Ba(Zr_{0.05}Ti_{0.95})_{1-x}(Fe_{0.5}Ta_{0.5})_xO_3$ ceramics. Materials Research Bulletin, 2015, 69, 36–40.

[19] Gouitaa, N, Lamcharfi, T, Bouayad, Mf, Abdi, F, Echatoui, N.S and Hadi, N. Dielectric anomalies of $BaTi_{1-x}Fe_xO_3$ ceramics for x = 0.0 to 0.6 of Fe doping concentration. Asian Journal of Chemistry, 2017, vol. 29, no. 10, 2143-2148.

[20] Rani, A, Kolte, J, Vadla, S.S, Gopalan, P. Structural, electrical, magnetic and magnetoelectric properties of Fe doped BaTiO3 ceramics. Ceramics International, 2016, 42, 8010–8016.

[21] Puli, V. S, Kumar, A, Chrisey, D. B, Tomozawa, M, Scott, J. F, Katiyar, R. S. Barium zirconate-titanate/barium calcium-titanate ceramics via sol–gel process: novel high- energy-density capacitors. J. Phys. D: Appl. Phys., 2011, 44, 395-403.

[22] Elbasset, A, Abdi, F, Lamcharfi, T, Sayouri, S, Abarkan, M, Echatoui, N. S and Aillerie, M. Influence of Zr on Structure and Dielectric Behavior of $BaTiO_3$ Ceramics. Indian Journal of Science and Technology, July 2015, 0974-5645.

[23] Bourguiba, F, Dhahri, Ah, Tahri, T, Dhahri, J, Abdelmoula, N, Taibi, K, Hlil, E.K. Structure properties and relaxor characteristics of the phases transformation in $BaTi_{0.5}(Fe_{0.33}Mo_{0.17})O_3$ perovskite ceramic. Journal of Alloys and Compounds, 2016, 675, 174-182.

[24] Zhang, Q, Wang, L, Luo, J, Tang, Q, Du, J. Structural and dielectric properties of $Bi(Mg_{1/2}Ti_{1/2})O_3$-$BaTiO_3$ lead-free ceramics, J. Am. Ceram. Soc, 2009, 92, 1871.

[25] Yang, Z, Chang, Y, Liu, B, Wei, L, Mater, J. Effect of composition on phase structure, microstructure and electrical properties of $(K_{0.5}Na_{0.5})$ NbO_3-$LiSbO_3$. Sci. Eng. A., 2006, 432, 292–298.

[26] Katiyar, R. S, Dixit, A, Majumder, S. B, and Bhalla, A. S. Effect of Zr Substitution for Ti on the Dielectric and Ferroelectric Properties of Barium Titanate Thin Films. Integrated Ferroelectrics, 2005, 70(1), 45–59.

[27] Ramesh, M.N.V, Ramesh, K.V. Structural, dielectric and AC conductivity studies on 0.8 $Ba_{0.2}(Bi_{0.5}K_{0.5})Ti_{1-x}Zr_xO_3$ lead free ceramic system. Materials Science-Poland, 2016, 34(3), 669-675.

[28] Dwivedi, R.K, Kumar, D, Prakash, O. Dielectric relaxation in valence compensated solid solution $Sr_{0.65}La_{0.35}Ti_{0.65}Co_{0.35}O_3$. J. Phys. D: Appl. Phys, 2000, 33- 88.

[29] Chung, C.Y, Chang, Y.S, Chen, G.J, Chung, C.C, Huang, T.W. Effects of bismuth doping on the dielectric properties of $Ba(Fe_{0.5}Nb_{0.5})O_3$ ceramic. Solid State Commun, 2008, 145, 212–217.

[30] Liao, K.F, Chang, Y.S, Chai, Y.L, Tsai, Y.Y. Structure and dielectric properties of sodium-doped $Ba(FeNb)_{0.5}O_3$. Chen. Mater.Sci.Eng., 2010, B172, 300.

[31] Yoon, K.H, Kim, D.P, Kim, E.S, Am, J. Effect of $BaWO_4$ on the microwave dielectric properties of $Ba(Mg_{1/3}$ $Ta_{2/3})O_3$. J. Am. Ceram. Soc, 1994, 77, 1062.

[32] Intatha, U, Eitssayeam, S, Wang, J, Tunkasiri, T. Impedance study of giant dielectric permittivity in $BaFe_{0.5}Nb_{0.5}O_3$ perovskite ceramic. Curr. Appl. Phys, 2010, 10-21.

[DOI: 10.22068/ijmse.2059]